PLOS CLIMATE

RESEARCH ARTICLE

# Changing temperature profiles and the risk of dengue outbreaks

**Imelda Trejo[1], Martha Barnard[2], Julie A. Spencer[2,3], Jeffrey Keithley[2,4], Kaitlyn M. Martinez[2], Isabel Crooker[2], Nicolas Hengartner[1,5], Ethan O. Romero-Severson[1], Carrie Manore[1]***

**1** T-6 Theoretical Biology and Biophysics, Los Alamos National Laboratory, Los Alamos, NM, United States of America, **2** A-1 Information Systems and Modeling, Los Alamos National Laboratory, Los Alamos, NM, United States of America, **3** Intelligence Community Postdoctoral Research Fellowship Program, Los Alamos National Laboratory, Los Alamos, NM, United States of America, **4** Department of Computer Science, University of Iowa, Iowa City, IA, United States of America, **5** Center for Nonlinear Studies, Los Alamos National Laboratory, Los Alamos, NM, United States of America

* cmanore@lanl.gov





**Citation:** Trejo I, Barnard M, Spencer JA, Keithley J, Martinez KM, Crooker I, et al. (2023) Changing temperature profiles and the risk of dengue outbreaks. PLOS Clim 2(2): e0000115. https://doi.org/10.1371/journal.pclm.0000115

**Editor:** Samuel Nii Ardey Codjoe, University of Ghana, GHANA

**Received:** January 24, 2022

**Accepted:** December 21, 2022

**Published:** February 15, 2023



**Data Availability Statement:** All data used in this analysis are publicly available. Details are provided in S1 Table.

**Funding:** IT and NH were funded by the Laboratory Directed Research and Development Program of Los Alamos National Laboratory under project numbers 20210709ER and 20210043DR. IT, MB, JK, KMM, IC, EOR, and CM were funded by the Laboratory Directed Research and Development Program of Los Alamos National Laboratory under project number 20210062DR. NH benefited from the support and resources of the Center for Non-

## Abstract

As temperatures change worldwide, the pattern and competency of disease vectors will change, altering the global distribution of both the burden of infectious disease and the risk of the emergence of those diseases into new regions. To evaluate the risk of potential summer dengue outbreaks triggered by infected travelers under various climate scenarios, we develop an SEIR-type model, run numerical simulations, and conduct sensitivity analyses under a range of temperature profiles. Our model extends existing theoretical frameworks for studying dengue dynamics by introducing temperature dependence of two key parameters: the mosquito extrinsic incubation period and the lifespan of mosquitoes, which empirical data suggests are both highly temperature dependent. We find that changing temperature significantly alters dengue risk in an inverted U-shape, with temperatures in the range 27-31˚C producing the highest risk. As temperatures increase beyond 31˚C, the determinants of dengue risk begin to shift from mosquito biting rate and carrying capacity to the duration of the human infectious period, suggesting that changing temperatures not only alter dengue risk but also the potential efficacy of control measures. To illustrate the role of spatial and temporal temperature heterogeneity, we select five US cities where the primary dengue vector, the mosquito *Aedes aegypti*, has been observed, and which have had dengue cases in the past: Los Angeles, Houston, Miami, Brownsville, and Phoenix. Our analysis suggests that an increase of 3˚C leads to an approximate doubling of the risk of dengue in Los Angeles and Houston, but a reduction of risk in Miami, Brownsville, and Phoenix due to extreme heat.

## Introduction

The global reported incidence of Dengue fever, a mosquito-borne disease caused by dengue virus [1], has increased 8-fold in the past two decades. Almost half of the world's population is

Linear Studies at LANL. JAS was supported by an appointment to the Intelligence Community Postdoctoral Research Fellowship Program at Los Alamos National Laboratory administered by Oak Ridge Institute for Science and Education (ORISE) through an interagency agreement between the U. S. Department of Energy and the Office of the Director of National Intelligence (ODNI). The findings and conclusions in this report are those of the authors and do not necessarily represent the official position of Los Alamos National Laboratory. Los Alamos National Laboratory, an affirmative action/equal opportunity employer, is managed by Triad National Security, LLC, for the National Nuclear Security Administration of the U.S. Department of Energy under contract 89233218CNA000001. The funders had no role in study design, data collection and analysis, decision to publish, or preparation of the manuscript.

**Competing interests:** The authors have declared that no competing interests exist.

now at risk [2], with an estimated 390 million new cases every year [3]. No effective vaccine is broadly available [4], and the primary way to mitigate the disease is through control of or protection from mosquito populations [5–7]. Mosquitoes are a necessary intermediate host for the dengue life-cycle. Mosquitoes are ectothermic, and their life cycle is very sensitive to environmental temperature, which is a key driver of annual dengue case counts [8–13].

The extrinsic incubation period (EIP) is the period from when a mosquito ingests an infectious blood meal to when it becomes infectious (competent to transmit dengue virus). As temperature increases, EIP decreases up to a point, suggesting a proportional relationship between temperature and dengue risk. However, for transmission to take place, the mosquito lifespan, which declines with increasing temperature after a certain point, must exceed the EIP [9, 13–17]. Recent work has quantified the impact of EIP dependence on temperature [14, 18–20].

Considerable modeling work has been done on the effects of temperature dependence of mosquito life traits on arbovirus transmission [21–25]. Mayton et al. established the importance of mosquito age structure on transmission potential, which we include in our model as a temperature dependent lifespan [26]. As temperature changes, the implicit age structure of the mosquito population also changes. Previous models have adopted varied approaches to studying the effects of temperature dependent parameters on disease dynamics. Mordecai et al. integrated multiple temperature dependent parameters to study the relationship of temperature on the epidemic threshold [21], while Kamiya et al. used an explicit epidemic model to examine the effect of temperature dependent EIP while fixing other model parameters [18]. Our study extends these approaches by allowing both lifespan and EIP to vary with temperature in a explicit mechanistic model that both allows us to simulate dynamics and define the epidemic threshold. This approach allows us to characterize temperature-dependent dengue risk more fully by including key drivers of the life-history trade-offs for both dengue and its mosquito hosts. The effects of a changing climate on mosquito-borne disease are not monotonic, and increasing temperatures can have complex effects not only the global distribution of dengue but also on mitigation strategies [13, 18, 21, 27].

Endemic dengue has been historically limited to tropical climates, since *A. aegypti* cannot survive below 8˚C [28]. However, single dengue outbreaks initiated by infected travelers have recently been confirmed in temperate regions [10, 29, 30]. Outbreaks are possible in cities with warm summers and mild winters near the northern borders of *A. aegypti* ranges. We have chosen to study the potential for outbreaks in two groups of U.S. cities that together represent a range of mean temperatures from 20.6˚C to 31.8˚C: (1) those where the mosquitoes are found, and limited outbreaks have occurred from imported cases in travelers (Los Angeles, Houston, and Phoenix) [31]; and (2) those where the mosquitoes are found, and autochthonous (locally transmitted) outbreaks have occurred (Miami, Brownsville) [31, 32]. The impact of rising temperatures on the risk of dengue outbreaks in the southern United States is an open question.

To explore this question, we adapt the mathematical models developed in [7, 33] to include temperature dependence of the EIP and mosquito lifespan parameters. Our model is composed of ordinary differential equations that describe the time evolution of an outbreak of dengue between humans and adult female mosquitoes. We consider a range of scenarios characterized by different temperatures and initial conditions to understand how temperature affects both dengue risk and mitigation. We compute four *quantities of interest* (QOIs) to evaluate disease invasion potential, transience and severity of outbreaks: (1) the basic reproduction number; (2) the final epidemic size; (3) the timing of the epidemic peak; and (4) the magnitude of the epidemic peak. We compare and evaluate not only the impact of temperature-dependent mosquito lifespan and EIP, but also how the uncertainty in these values impacts disease dynamics and global parameter sensitivity. It then becomes possible to provide a spectrum of possible disease outcomes under a range of climate change scenarios.

# Materials and methods

## Model development

We model the time evolution of a single dengue outbreak in a location without endemic dengue transmission using a compartmental model that tracks human and mosquito populations. The model assumes that the human population is large enough such that mosquitoes are not limited by blood meal availability and the outbreak period is short enough that the total human population remains constant.

The model (Fig 1) divides the total human population, $N_h$, into four classes: susceptible $S_h$, exposed $E_h$, infectious $I_h$ and recovered $R_h$. The susceptible humans, $S_h$, move to the exposed class when the human become infected by the bite of an infectious mosquito. Exposed humans, $E_h$, move to the infectious class, $I_h$, in which humans can infect mosquitoes. Infectious humans, $I_h$, recover and move to the recovered class, $R_h$. Importantly, our exposed class is comprised of the persons who were infected but not yet infectious. We model the exposed period (latent period) with the intrinsic incubation period (IIP), which is often inferred from the time between a human being infected to having detectable virus [14, 34]. Given that our model is only applicable to a single outbreak, we assume that recovered humans acquire immunity to the dengue virus for the given season [35, 36].

The total mosquito population, $N_v$, is divided in three classes: susceptible $S_v$, exposed $E_v$, and infectious $I_v$. We assume that mosquitoes enter the susceptible class through birth and that all female mosquitoes are born susceptible. Then susceptible mosquitoes move to the exposed class $E_v$ via biting a dengue infected human. Exposed mosquitoes move to the infectious class $I_v$ after completing their extrinsic incubation period, where they remain for the rest of their natural life. We assume that dengue infection does not affect the lifespan of a mosquito. The demographics of the mosquito population follow a logistic growth pattern, i.e. the mosquito birth rate decreases linearly as the populations' size approach a constant carrying capacity $K_v$ controlled by the availability of egg-laying sites and competition between larvae [7].

Following the flow diagram given in Fig 1 and the modeling assumptions described above yields the system of equations:

$$\frac{dS_h}{dt} = -\lambda_h(t)S_h \tag{1}$$

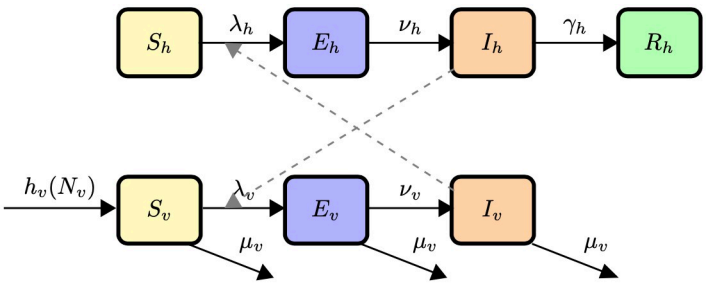


**Fig 1. Model diagram.** Compartmental diagram for dengue virus transmission and subsequent disease progression across humans and mosquitoes. Susceptible human $S_h$ become exposed to dengue, $E_h$, by the bite of an infectious mosquito $I_v$. Exposed persons become infectious, $I_h$, after an incubation period, after which they are removed, $R_h$, once the infection is cleared. Susceptible mosquitoes, $S_v$, enter the system at the rate $h_v(N_v)$ where they either die or become exposed, $E_v$, when they bite an infected person. Exposed mosquitoes become infectious, $I_v$, after the EIP and leave the system though natural death.

https://doi.org/10.1371/journal.pclm.0000115.g001

$$\frac{dE_h}{dt} = \lambda_h(t)S_h - v_h E_h \tag{2}$$

$$\frac{dI_h}{dt} = v_h E_h - \gamma_h I_h \tag{3}$$

$$\frac{dR_h}{dt} = \gamma_h I_h \tag{4}$$

$$\frac{dS_v}{dt} = h_v(N_v)N_v - \lambda_v(t)S_v - \mu_v S_v \tag{5}$$

$$\frac{dE_v}{dt} = \lambda_v(t)S_v - v_v E_v - \mu_v E_v \tag{6}$$

$$\frac{dI_v}{dt} = v_v E_v - \mu_v I_v. \tag{7}$$

The total population sizes are $N_h = S_h + E_h + I_h + R_h$ and $N_v = S_v + E_v + I_v$. The mosquito birth rate is [7]:

$$h_v(N_v) = \Psi_v - \frac{r_v}{K_v}N_v, \tag{8}$$

where $\Psi_v$ is the natural birth rate in the absence of density dependence, $r_v = \Psi_v - \mu_v$ is the intrinsic growth rate of mosquitoes in the absence of density dependence, and $K_v$ is the carrying capacity of mosquitoes in the region considered.

The forces of infection from mosquito to humans, $\lambda_h(t)$, and from human to mosquitoes, $\lambda_v(t)$, are [33, 37]:

$$\lambda_h(t) = \frac{a_v N_v}{N_h} \cdot \beta_{hv} \cdot \frac{I_v}{N_v} = \frac{a_v \beta_{hv} I_v}{N_h} \quad \text{and} \quad \lambda_v(t) = \frac{a_v \beta_{vh} I_h}{N_h}, \tag{9}$$

under the assumption that mosquitoes are not limited by available blood meals. $a_v$ is the constant human-biting rate of the mosquitoes, which is defined as the average number of bites to humans by each mosquito per unit time; $\beta_{hv}$ is the infectivity of an infectious mosquito, which is defined as the probability of pathogen transmission from an infectious mosquito to a susceptible human given that a contact between the two occurs; $\beta_{vh}$ is the infectivity of an infectious human, which is defined as the probability of pathogen transmission from an infectious human to a susceptible mosquito given that a contact between the two occurs; $v_h$ is the average rate of time progression of humans from the exposed state to the infectious state; $\gamma_h$ is the average human recovery rate; $v_v$ is the average rate of time progression of mosquitoes from the exposed state to the infectious state; and $\mu_v$ is the mosquito per-capita natural death rate. Table 1 summarizes the model parameter descriptions and their units.

## Temperature-dependent parameters

We used previous models and data reported from the literature to estimate the temperature dependence in the EIP and lifespan parameters for *A. aegypti* mosquitoes. The temperature-dependent parameter values and ranges for the EIP ($1/v_v$) were taken from the Bayesian log-normal time to event model fit by Chan and Johansson 2012 [14]. The mean value at each temperature is the mean of the posterior distribution and the 95% interval is the middle 95% of the

**Table 1. Model parameters and their units.**

| Parameters | Description | Units |
|---|---|---|
| $a_v$ | Human-biting rate of mosquitoes | 1/days |
| $\beta_{hv}$ | Infectivity of an infectious mosquito | dimensionless |
| $\beta_{vh}$ | Infectivity of an infectious human | dimensionless |
| $\gamma_h^{-1}$ | Average human infectious period | days |
| $\mu_v^{-1}$ | Average mosquito lifespan | days |
| $\nu_v^{-1}$ | Average extrinsic incubation period (EIP) | days |
| $\nu_h^{-1}$ | Average intrinsic incubation period (IIP) | days |
| $\Psi_v$ | Per capita recruitment rate of mosquitoes | 1/days |
| $K_v$ | Carrying capacity of mosquitoes | mosquitoes |
| $H_0$ | Total human population size | humans |

https://doi.org/10.1371/journal.pclm.0000115.t001

posterior distribution as presented in Tables 2 and 3. These values were explicitly provided for 25˚C and 30˚C. For 20˚C, 35˚C, and the temperatures of the three United States cities of interest, these values were estimated from figures. For mosquito lifespan ($1/\mu_v$), we compiled temperature lifespan data on *A. aegypti* from various studies at temperatures greater than or equal to 15˚C [38–40]. We then fit generalized linear models to the data, using the four distributions explored by [14], namely, lognormal, gamma, Weibull, and exponential (see S1 Table for more details). We explored explanatory variables up to degree five polynomials of temperature for all models; however, we used a degree three temperature polynomial for all model types, based on Likelihood Ratio Tests between nested models. All four model types fit the data to a similar extent: a different model performed the best for each of Akaike Information Criteria (AIC) and mean squared error (MSE), and the AIC values were within 20 units of each other. Therefore, we selected the Gamma regression fit for simplicity. We used the prediction from the Gamma regression at a given temperature as the mean parameter value. We then calculated a 95% prediction interval of the modeled mosquito lifespan at every temperature of interest using the method developed by [41]. We summarized these values in Tables 2 and 3 at each temperature of interest.

The 2021 mean temperatures for Los Angeles, Houston, Miami, Brownsville, and Phoenix over June-October were 20.6˚C, 27.7˚C, 28.4˚C, 28.9˚C, and 31.8˚C respectively (Table 3). Monthly temperatures were obtained from [42].

## Stability analysis

We mathematically analyzed Model (1)–(7) to define the conditions under which the model describes feasible dengue outbreaks and to find the equilibria of the system and their

**Table 2. Parameter values for the EIP and mosquito lifespan by temperature.**

| Temperature | Average EIP ($\nu_v^{-1}$) | | Average lifespan† ($\mu_v^{-1}$) | | Reference |
|---|---|---|---|---|---|
| | Mean | 95% Interval | Mean | 95% Interval | |
| 20˚C | 20.0 | [9, 39.1] | 24.9 | [14.6, 38.6] | [14], S1 Table |
| 25˚C | 15.0 | [5.0, 33.0] | 30.1 | [17.7, 46.2] | [14], S1 Table |
| 30˚C | 6.5 | [2.4, 15.0] | 27.6 | [16.2, 42.4] | [14], S1 Table |
| 35˚C | 5.5 | [2, 12] | 11.2 | [6.4, 17.8] | [14], S1 Table |

† Parameter values estimated in this work

https://doi.org/10.1371/journal.pclm.0000115.t002

**Table 3. Temperature-dependent parameter values for five United States cities.**

| Temperature | Average EIP ($\nu_v^{-1}$) | | Average lifespan† ($\mu_v^{-1}$) | | Reference |
|---|---|---|---|---|---|
| | Mean | 95% Interval | Mean | 95% Interval | |
| Los Angeles 20.6˚C* | 19.0 | [8.5, 38.0] | 24.5 | [14.8, 39.4] | [14], S1 Table |
| Houston 27.7˚C* | 11.0 | [3.0, 22.0] | 30.8 | [18.1, 47.2] | [14], S1 Table |
| Miami 28.4˚C* | 9.5 | [3.3, 19.5] | 30.2 | [17.7, 46.4] | [14], S1 Table |
| Brownsville 28.9˚C* | 8.0 | [2.8, 18.5] | 29.6 | [17.4, 45.5] | [14], S1 Table |
| Phoenix 31.8˚C* | 6.0 | [2.3, 14.0] | 22.5 | [13.2, 34.6] | [14], S1 Table |

* Average temperature from June-October 2021.

† Parameter values estimated in this work

https://doi.org/10.1371/journal.pclm.0000115.t003

corresponding stability properties. Each equilibrium provides a possible outcome of the dengue outbreak and its corresponding stability properties define the conditions under which a particular result occurs.

In the S1 Appendix, we proved that Model (1)–(7) is epidemiologically and mathematically well-defined in the domain $\mathcal{D} = \{(S_h, E_h, I_h, R_h, S_v, E_v, I_v) \in \mathbb{R}^7 : 0 \leq S_h, E_h, I_h, R_h \leq H_0,\ 0 \leq S_v, I_v, E_v \leq K_v,\ H_0 = S_h + E_h + I_h + R_h \text{ and } S_v + I_v + E_v \leq K_v\}$ and that for any initial condition in $\mathcal{D}$ there is a unique solution of System (1)–(7) which remains in $\mathcal{D}$ for all time $t > 0$. Setting the right-hand sides of the Eqs (1)–(7) equal to zero yields the two equilibria:

$$x_0^* = (S_h^*, 0, 0, R_h^*, 0, 0, 0) \quad \text{and} \quad x_1^* = (S_h^*, 0, 0, R_h^*, K_v, 0, 0),$$

where $S_h^*$ and $R_h^*$ are any two real numbers. The two equilibrium points have biological meaning when $x_0^*$ and $x_1^*$ are in $\mathcal{D}$, i.e., $0 \leq S_h^* \leq H_0$, $0 \leq R_h^* \leq H_0$ and $R_h^* = H_0 - S_h^*$. The two points $x_0^*$ and $x_1^*$ are both disease-free equilibria, i.e., $I_h^* = 0$, $E_h^* = 0$, $E_v^* = 0$ and $I_v^* = 0$. However, in the steady state $x_0^*$ the mosquito population dies out $S_v^* = 0$; while in the steady state $x_1^*$ the mosquitoes achieve their maximal population size $K_v$. The following theorems provide the corresponding stability properties of each steady state. We provide their proofs in the S1 Appendix.

**Theorem 1**. *Suppose that $R_h^* = H_0 - S_h^*$ and $H_0 \geq S_h^* \geq 0$. Then $x_0^* = (S_h^*, 0, 0, R_h^*, 0, 0, 0,)$ exists for all the parameter values and $x_0^*$ is unstable.*

**Theorem 2**. *Suppose that $R_h^* = H_0 - S_h^*$ and $H_0 \geq S_h^* \geq 0$. Then $x_1^* = (S_h^*, 0, 0, R_h^*, K_v, 0, 0)$ exists for all the parameter values and $x_1^*$ belongs to the set $X_s = \{(H_0 - R_h, 0, 0, R_h, K_v, 0, 0): 0 \leq R_h \leq H_0\}$, which is a local attractor set of the solution set given by System (1)–(7) when $\mathcal{R}_0 < 1$. $x_1^*$ is unstable when $\mathcal{R}_0 > 1$, where*

$$\mathcal{R}_0 = \frac{\nu_v}{\mu_v + \nu_v} \cdot \frac{a_v \beta_{vh}}{\gamma_h H_0} K_v \cdot \frac{a_v \beta_{hv}}{\mu_v} \frac{S_h^*}{H_0}. \tag{10}$$

The threshold value $\mathcal{R}_0$ is known as the basic reproduction number. The $\sqrt{R_0}$ is often interpreted as the expected number of human to mosquito or mosquito to human secondary cases [7, 43]. Here, $\mathcal{R}_0$ characterizes the stability of the disease free equilibrium $x_1^*$ which is unstable and an outbreak occurs when $\mathcal{R}_0 > 1$. In this case, the infective curve $I_h(t)$ first increases from an initial $I_h(0)$ near zero, reaches a peak, and then decreases toward zero as a function of time [44]. As time goes to infinity, the final epidemic size is $R_h^* = H_0 - S_h^*$ which satisfies $0 \leq R_h^* \leq H_0$.

We expressed $\mathcal{R}_0$ in three terms. The first term, $\nu_v/(\mu_v + \nu_v)$, is the probability that an exposed mosquito will survive the extrinsic incubation period. The second term, $a_v\beta_{vh}K_v/$

($\gamma_h H_0$), is the average number of newly infections that result from human to mosquito. The third term, $a_v \beta_{hv} S_h^* / (\mu_v H_0)$, is the average newly infections that result from mosquito to human.

## Sensitivity analysis

We employed two sensitivity analysis methods: Latin Hypercube Sampling (LHS) and the extended Fourier Amplitude Sensitivity Test (eFAST), to quantify the relative impact of model parameter uncertainties on the *quantities of interest* (QOIs): basic reproduction number ($\mathcal{R}_0$), epidemic peak and final epidemic size. All sensitivity analysis was performed through numerical simulations at 20˚, 25˚, 30˚C, and 35˚ temperature scenarios, from day 0 to 1500 (time relatively large that numerically the disease die out at and beyond of it).

For the Latin Hypercube Sampling [45], we used a uniform distribution to generate 10,000 sampled sets from the parameter space of EIP ($1/\nu_v$) and mosquito lifespan ($1/\mu_v$) (Table 2). From these sampled sets, we computed the basic reproduction number ($\mathcal{R}_0$) across these parameters and explored at what temperatures the relationship between EIP ($1/\nu_v$) and mosquito lifespan ($1/\mu_v$) parameters yielded non-epidemic scenarios ($\mathcal{R}_0 < 1$).

For the eFAST method [46], we generated 1,000 samples for each parameter and computed the sensitivity indices of the epidemic peak and final epidemic size. We varied all the parameters in Table 1 simultaneously within the range of values as presented in Tables 2 and 4. We excluded the parameter $H_0$ in our analysis, despite its impact on the vector-to-host and total susceptible ratios and therefore our QOIs. The qualitative behaviors of the sensitivity indices are both similar when varying or fixing $H_0$, as we assumed that $K_v$ increases proportionally with $H_0$ and both parameters have the same order of magnitude (the numerical results are not presented in this work). Additionally, we excluded $H_0$ because we aimed to explore the variability of the QOI to parameters that could be altered through interventions, such as mosquito repellent and reducing vector populations, in order to mitigate disease spread. The resulting magnitudes of the sensitivity indices from the eFAST determine the importance of the parameters on the QOI variability [46, 47]. Specifically, eFAST computes the first order and total order sensitivity indices. The first order sensitivity index represents the fractional contribution of a single parameter to the QOI variance, while the total order sensitivity index takes into account parameter interactions. The difference between the total order and first order is the interaction order sensitivity index, which represents the sole impact of non-linear interactions between parameters on QOI variance. The higher the sensitivity indices are for a given parameter, the larger the influence that parameter exerts on the variance of the QOI. We primarily examined the first order and interaction sensitivity indices for our QOIs, and presented results through visualizations of these metrics.

**Table 4. Non-temperature varying parameter values used in simulations.**

| Parameter | Baseline Value | Range | Reference |
|---|---|---|---|
| $a_v$ | 0.75 | [0.063, 1] | [7, 48] |
| $\beta_{hv}$ | 0.33 | [0.10, 0.75] | [7] |
| $\beta_{vh}$ | 0.33 | [0.10, 0.75] | [7] |
| $\gamma_h^{-1}$ | 6 | [4, 12] | [7] |
| $\nu_h^{-1}$ | 6.1 | [3, 14] | [7, 14] |
| $\Psi_v$ | 0.30 | [0.28, 0.32] | [7] |
| $K_v$ | $\frac{1}{2}H_0$ | $\left[\frac{1}{4}H_0, H_0\right]$ | [7, 49] |
| $H_0$ | $1 \times 10^5$ | $[1 \times 10^4, 2 \times 10^5]$ | [7, 50] |

https://doi.org/10.1371/journal.pclm.0000115.t004

### Numerical simulations of single outbreaks

We used our model to numerically simulate summer dengue outbreaks at the current mean temperature and at a 3˚C temperature increase over June-October for Los Angeles, Houston, Miami, Brownsville, and Phoenix (Table 3). To evaluate the effects of temperature on the risk of dengue outbreaks for these cities, we computed the four QOIs for each city's simulated outbreaks. Note that to capture the seasonality of the mosquitoes and obtain realistic final epidemic sizes we set the mosquito natural birth rate ($\psi_v$) to zero after 180 days into the simulation. Each QOI was computed from simulated outbreaks using the mean values for all parameters. To present the range of possible QOIs in each United States city, we also calculated the QOIs at combined maximum and minimum values of EIP and mosquito lifespan from the 95% intervals, with all other parameters at their mean values. Namely, we examined the following combinations: the largest EIP and smallest lifespan (lowest possible disease spread) and the smallest EIP and largest lifespan (highest possible disease spread) (Table 3) for a particular mean temperature.

In all numerical simulations and sensitivity analyses, we used the parameter values in Table 4 and all initial conditions are zero except $I_h(0) = 1$, $S_h(0) = H_0 - 1$, and $S_v(0) = K_v$, with $H_0 = 1 \times 10^5$ for the sensitivity analysis and $H_0$ being approximations for the 2020 populations for the five United States cities (Los Angeles: 13,109,903; Houston: 7,154,478; Miami: 6,138,333; Brownsville: 421,017; Phoenix: 5,059,909) [51].

## Results

### Impact of temperature-dependent parameters on basic reproduction number

Fig 2 shows the value of $\mathcal{R}_0$ as a function of the range of values of EIP ($1/\nu_v$) and mosquito lifespan ($1/\mu_v$) consistent with a given temperature. Because $\mathcal{R}_0 \geq 1$ is the threshold criteria for an outbreak to occur, the overall inverted 'U' shaped effect of temperature on the probability of an outbreak is clear. At low temperatures (20˚C), much of the parameter range is not consistent with an outbreak; that is, at this temperature, our theory predicts relatively few outbreaks of small size. However, an increase of 10˚C leads to a nearly guaranteed outbreak scenario if dengue is present. Between 30˚C and 35˚C, the risk of an outbreak plummets to nearly zero due to the fact that almost all of the infected mosquitoes die before they become infectious. Overall, at all temperatures, mosquito lifespan has a stronger effect on $\mathcal{R}_0$ than EIP.

### Sensitivity of the epidemic peak and final outbreak size to parametric variance at different temperatures

Figs 3 and 4 show the sensitivity of the peak and final epidemic size to each parameter at 30˚C. Both QOIs show very similar patterns with the mosquito biting rate having the largest influence on both QOIs; 50–60% of variance in the QOIs is explained the variance in the biting rate and the interaction between biting rate and other parameters. One key difference in the sensitivity of the QOIs is that the peak epidemic size is much more sensitive to the human infectious period than is the final epidemic size. That is, interventions designed to shorten the period that infected humans are contagious are more effective at reducing the peak size of the epidemic, but less effective at reducing the overall risk. For both QOIs, the interaction of multiple parameters generally explains more of the variance than do the direct effects of most parameters, highlighting the non-linear nature of dengue transmission.

Temperature has a large effect on the sensitivity of the QOIs to parametric variance (Fig 5). As expected, the parameters with direct temperature variability display differential effects on

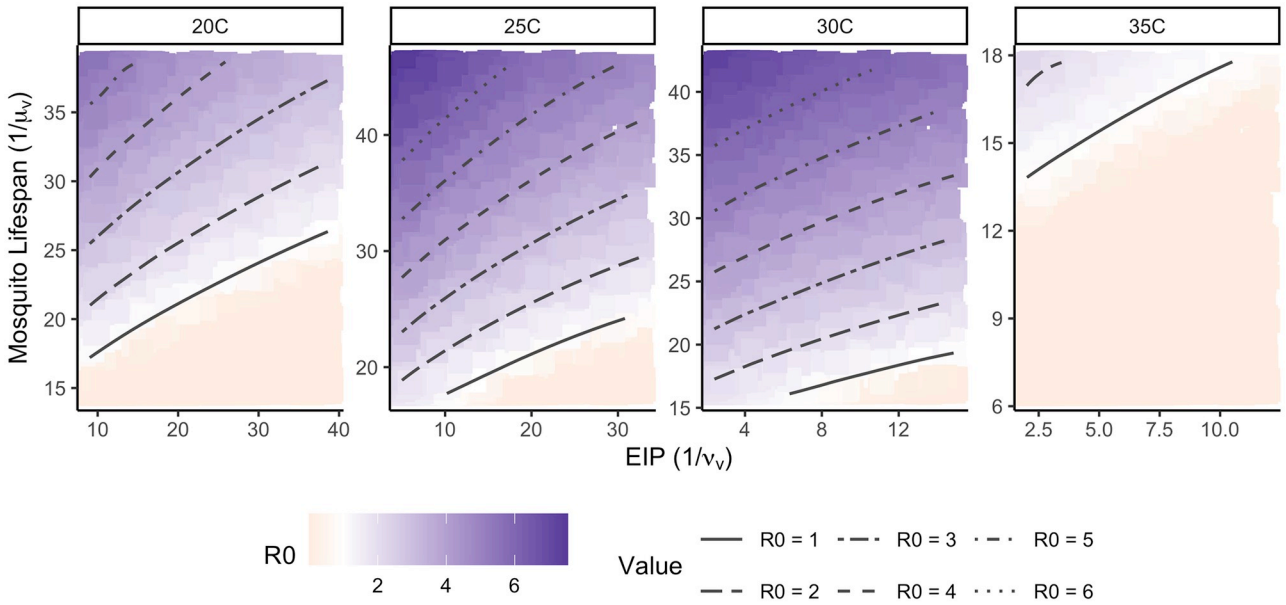


**Fig 2. Impact of EIP and mosquito lifespan on $\mathcal{R}_0$.** This figure shows the basic reproduction number ($\mathcal{R}_0$) for the possible values of EIP ($1/\nu_v$) and mosquito lifespan ($1/\mu_v$) at 20˚C, 25˚C, 30˚C, and 35˚C. Note that since possible ranges of these parameter values differ by temperature (Table 3), the horizontal and vertical axes vary by panel. At 35˚C, there is the largest proportion of the parameter space that yields non-outbreak scenarios. At both 25˚C and 30˚C, the majority of possible EIP and mosquito lifespan values generate $\mathcal{R}_0 \geq 1$ such that an outbreak occurs.

https://doi.org/10.1371/journal.pclm.0000115.g002

the QOIs at different temperatures. Consistent with the $\mathcal{R}_0$ analysis, the role of the mosquito lifespan on the QOIs is much higher at temperatures greater than 30˚C because the mosquito lifespan drastically decreases at these temperatures. Above 30˚C, the infectious mosquitoes may die before they become infectious and therefore there is a low probability of experiencing an outbreak at 35˚C. However, temperature also affects the role of parameters that do not directly have temperature-dependent forms. The impacts of the mosquito carrying capacity and human infectious period, which at 30˚C are shown to explain a significant proportion of the variance of the peak of infected humans, increase with temperature only up to 30˚C. While sensitivity analysis at a fixed temperature of 30˚C demonstrates that a very small proportion of the variance in the final epidemic size is due to the human infectious period (Fig 4), exploring across temperatures, we see that the sensitivity of the human infectious period nearly doubles at 35˚C. In contrast, the role of the mosquito carrying capacity on final epidemic size tends to decrease as temperature increases.

Generally, while the first order sensitivity of the QOIs to the EIP and mosquito lifespan decreases between 25˚C and 30˚C, the first order sensitivity of the QOIs to the human infectious period and mosquito carrying capacity increases. Temperatures between 25˚C and 30˚C also yield the largest dengue outbreaks (Figs 2 and 7).

## Effect of temperature on potential dengue dynamics in Los Angeles, Houston, Miami, Brownsville, and Phoenix

We examine simulated dengue outbreaks for five United States cities (Los Angeles, Houston, Miami, Brownsville, and Phoenix) at their current (2021) mean temperatures from June to October and at a 3˚C increase from the current mean temperature. Under the 3˚C increase (from (27.7˚ to 30.7˚C), Houston has the largest epidemic peak increase (Fig 6). Brownsville has the largest potential peak at current mean temperatures. With a 3˚C increase, Los Angeles

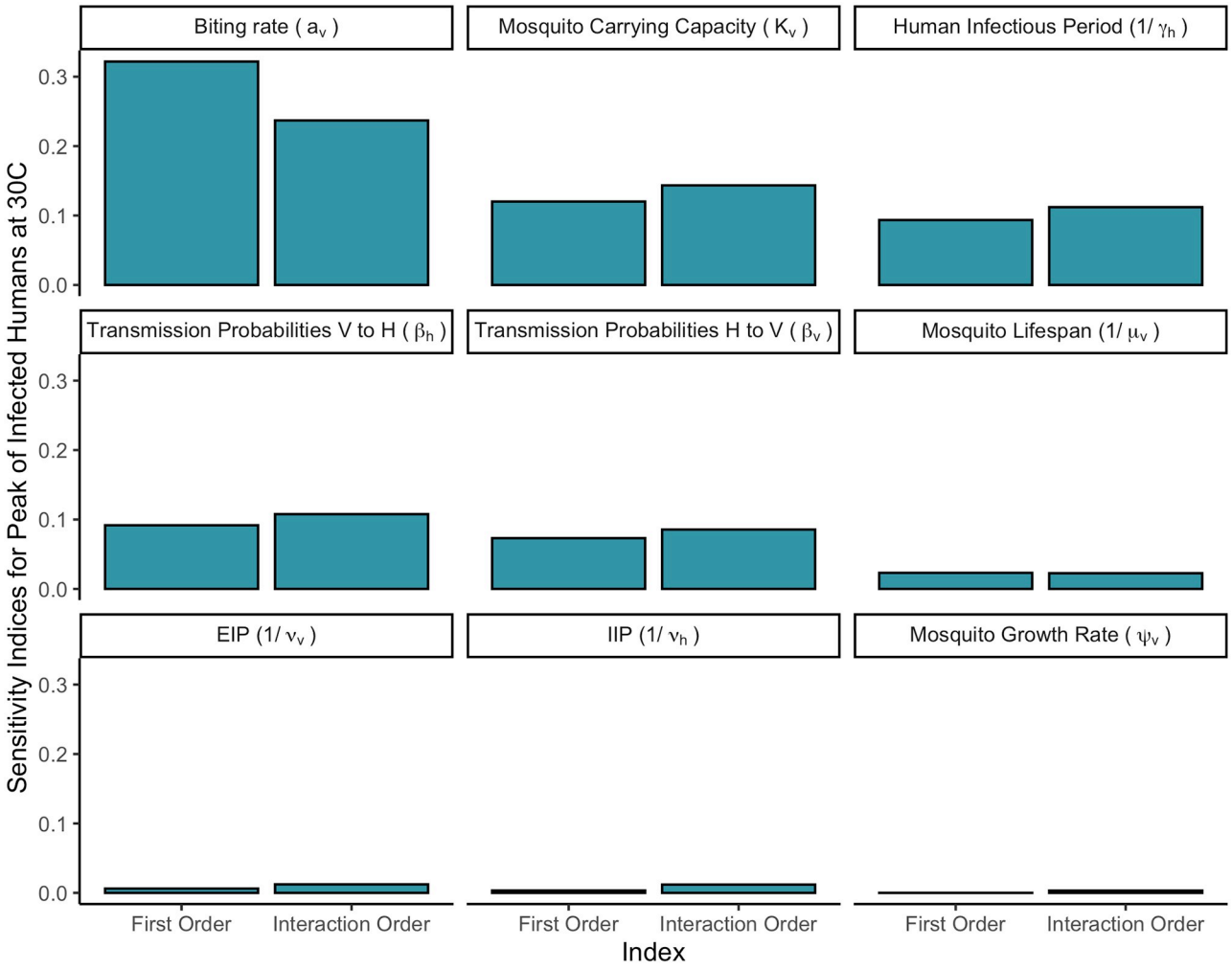


**Fig 3. Sensitivity of epidemic peak to parameters at 30˚C.** This figure shows the the first and interaction order sensitivity (horizontal axis) of epidemic peak to each parameter (panel). The peak of infectious humans is most sensitive to changes in the biting rate ($a_v$), mosquito carrying capacity ($K_v$), and human infectious period ($\gamma_h$).

https://doi.org/10.1371/journal.pclm.0000115.g003

and Houston's epidemic peaks increase and Miami and Brownsville's decrease, while an outbreak does not occur in Phoenix. Generally, temperature increases up to around 31˚ correspond to increased disease spread. However, temperatures higher than 31˚C lead to a decrease in disease spread, and by 35˚C there is no dengue outbreak. At the current temperatures, all five cities are at risk of a dengue outbreak, however cities with temperatures around 27–31˚C tend to have the largest outbreaks (as seen in Houston's simulated outbreaks).

Houston also has a higher simulated epidemic peak, final epidemic size, and basic reproduction number than either Los Angeles or Phoenix (Fig 7). In addition, Houston has the potential for a much larger epidemic peak and final epidemic size than do those cities, as demonstrated by the bars which represent the range of possible values. Los Angeles and Phoenix tend to have similar values for all QOIs except the time of epidemic peak, where Phoenix's epidemic peak occurs slightly earlier than Los Angeles'. However, Phoenix has the potential for a higher epidemic peak and final epidemic size than does Los Angeles. Of the cities, the simulated outbreak in Houston leads to the highest number of infected individuals.

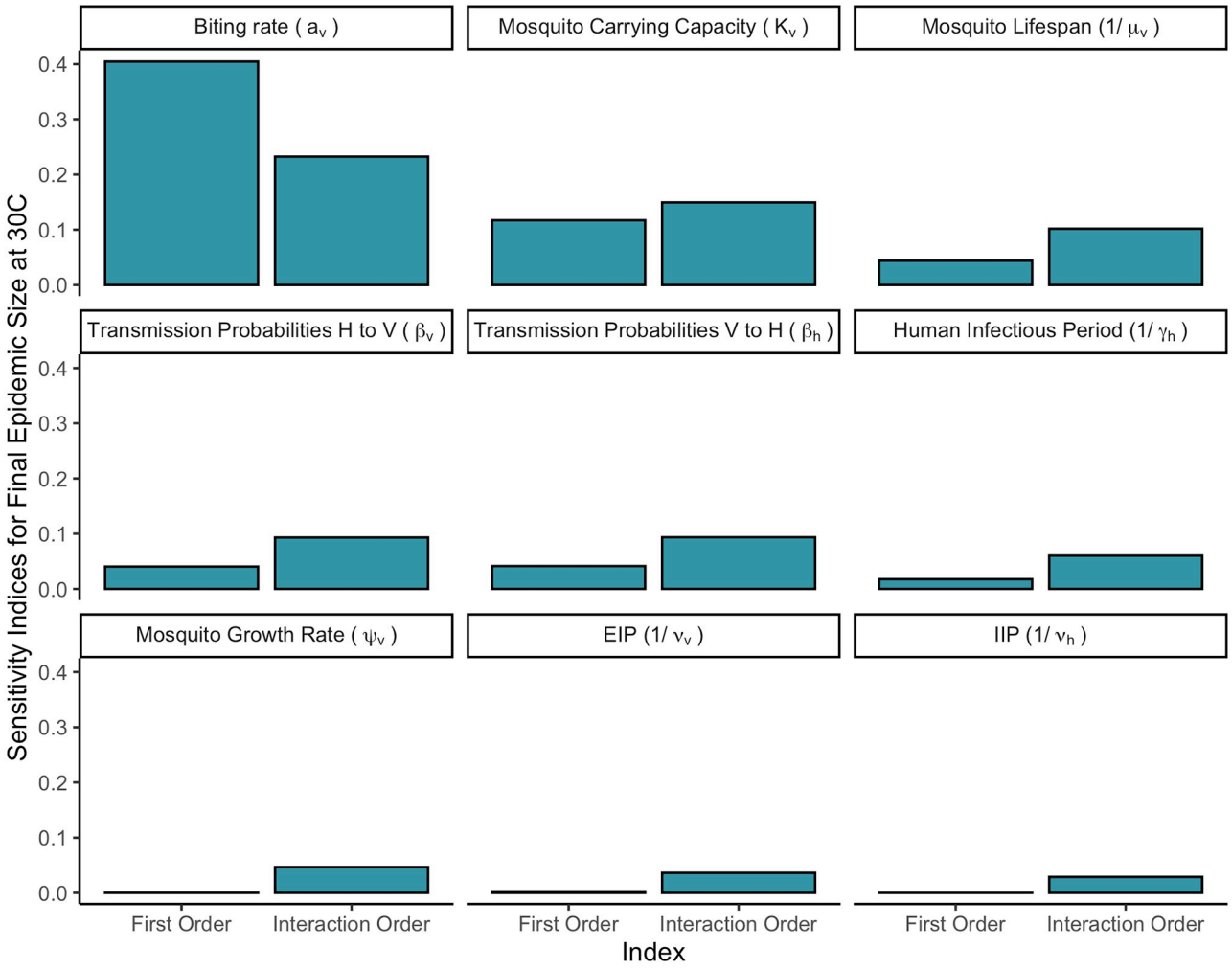


**Fig 4. Sensitivity of final epidemic size to parameters at 30˚C.** This figure shows the the first and interaction order sensitivity (horizontal axis) of final epidemic size to each parameter (panel). The final epidemic size is most sensitive to changes in the biting rate ($a_v$), mosquito carrying capacity ($K_v$), and mosquito lifespan ($1/\mu_v$).

https://doi.org/10.1371/journal.pclm.0000115.g004

## Discussion

We analyzed a standard mosquito-born disease model to quantify the impact of key temperature-dependent transmission parameters to dengue epidemic outbreaks in three United States cities. We found that all five cities explored (Los Angeles, Houston, Miami, Brownsville, Phoenix) are at risk of a dengue outbreak at their current average temperatures, and that Houston specifically has the highest risk of a large disease burden. With increasing temperatures due to climate change, Los Angeles and Houston could potentially see larger dengue outbreaks, while risk may decrease in Miami and Brownsville. The temperatures in Phoenix may become incompatible with a dengue outbreak. Furthermore, temperatures between 25˚C and 30˚C yield *A. aegypti* EIP and lifespan values that are most conducive to disease spread, while both lower and higher temperatures tend to generate smaller or no outbreaks. Of the explored parameters, changes in biting rate and mosquito carrying capacity have the largest influence on the variation of the number of infected humans. While the sensitivity of the majority of parameters do not vary by temperature, as temperature increases up to 30˚C, the sensitivity of

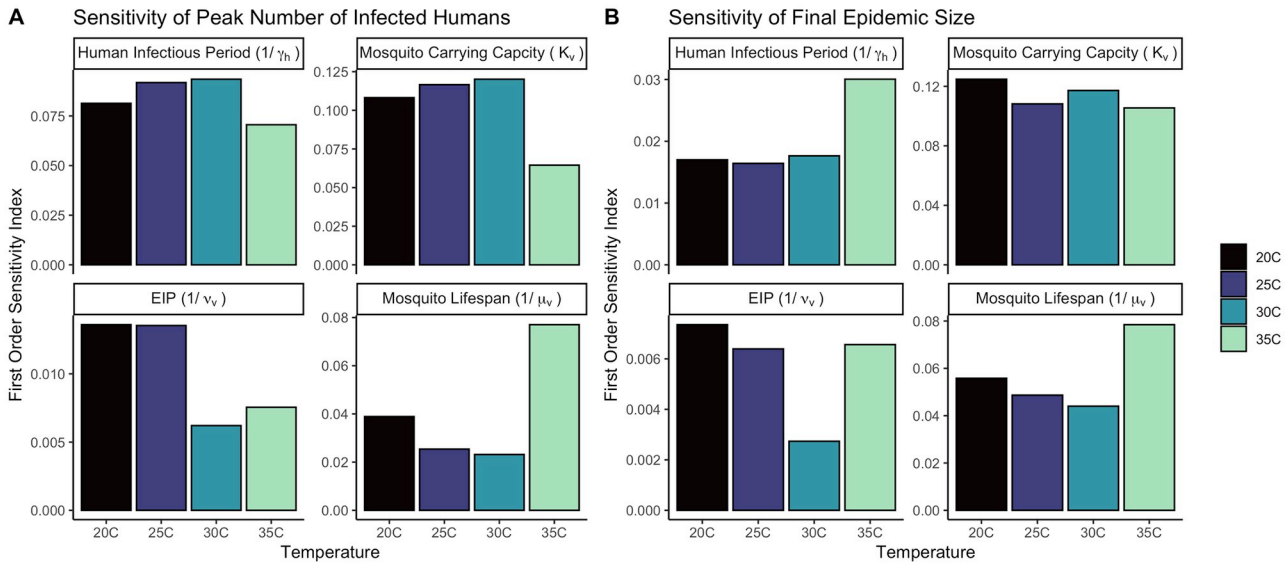


**Fig 5. Sensitivity of the QOIs to parameters varied by temperature.** This figure shows the first and interaction order sensitivity indices of both the peak number of infected humans (A) and final epidemic size (B) to parameters whose sensitivity varied by temperature. Between 20˚C and 30˚C, the sensitivity of the QOIs to EIP ($1/\nu_v$) and mosquito lifespan ($1/\mu_v$) decreases while the sensitivity of the QOIs to human infectious ($1/\nu_h$) and mosquito carrying capacity ($K_v$) tends to increase. First order sensitivity of the final epidemic size to all parameters except carrying capacity tends to be high at 35˚C.

https://doi.org/10.1371/journal.pclm.0000115.g005

the EIP and mosquito lifespan for the epidemic peak and final epidemic size tend to decrease, and the sensitivity of the human infectious period tends to increases.

Previous studies have supported the assertion that a shorter EIP can result in increased transmission [9, 17]. While our results generally agree with this conclusion, we also show that there is a trade off between EIP and mosquito lifespan. Between 25–30˚C, the EIP is small and mosquito lifespan is relatively large, and therefore larger and more quickly moving outbreaks occur at these temperatures. However, the EIP decreases as temperature increases, while adult mosquito lifespan also starts decreasing at 30˚C. Our model shows that at around 35˚C there is

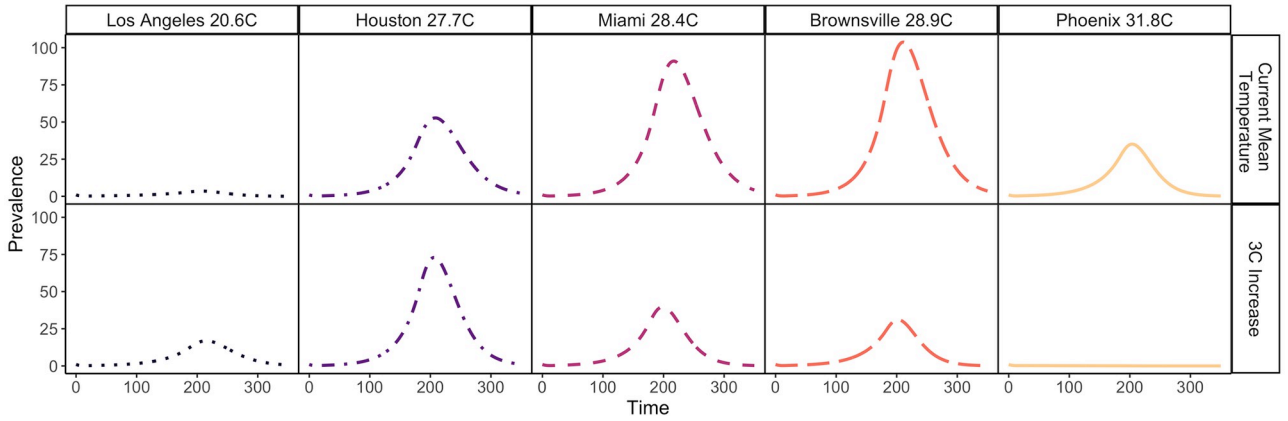


**Fig 6. Infected human dynamics for United States cities.** This figure depicts the possible epidemic trajectory of dengue in five United States cities at the current mean temperature from June-October for each city and at a 3˚C temperature increase from the current mean temperature. At current mean temperatures, fastest disease progression and highest numbers of infected humans are observed Houston, Miami, and Brownsville. With a 3˚C mean temperature increase, disease spread decreases for Miami and Brownsville, and is eliminated in Phoenix. In all cities, an outbreak occurs at the current mean temperature.

https://doi.org/10.1371/journal.pclm.0000115.g006

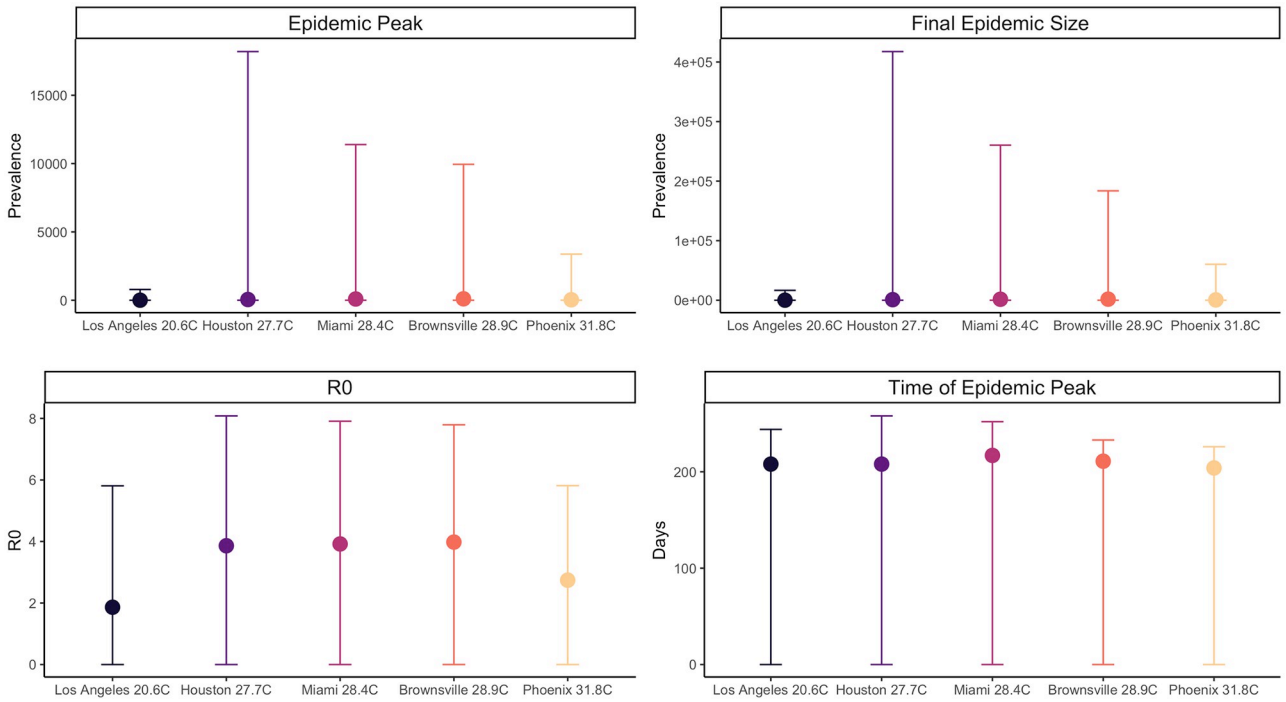


**Fig 7. Quantities of interest for United States cities.** This figure shows the epidemic peak, final epidemic size, basic reproduction number ($\mathcal{R}_0$), and time of epidemic peak for Los Angeles, Houston, Miami, Brownsville, and Phoenix. Error bars demonstrate the potential variation in the QOIs for each city. Houston has the potential for a much larger epidemic peak and final epidemic size than the other four cities. Houston, Miami, and Brownsville tend to have higher $\mathcal{R}_0$s than the other two cities. The QOIs of the simulated outbreaks for Los Angeles and Phoenix tend to take similar values.

https://doi.org/10.1371/journal.pclm.0000115.g007

a high probability that even if dengue is introduced, there would be no outbreak. Our sensitivity results also show that total interaction order sensitivity is larger than single order for the final epidemic size, and to a lesser extent, the peak. This indicates that temperature impacts on several parameters may serve as a multiplier to risk changes, having a larger impact than would be indicated by individual parameter sensitivity alone.

Our model also indicates where interventions may have the most relative benefit. Overall, our quantities of interest are most sensitive to the biting rate and mosquito carrying capacity. We should then target interventions at these two parameters (repellent to reduce bites, reducing mosquito density). Interestingly, between 25–30˚C, sensitivity of model output to EIP and mosquito lifespan decreases, while sensitivity to the human infectious period increases. This indicates that as temperatures increases within this range (the range of highest disease transmission), human interventions (such as quarantine or preventing onward transmission to mosquitoes) may become more important to limiting disease spread. Also, at higher temperatures, the QOIs are much more sensitive to mosquito lifespan, so reducing the mosquito lifespan can provide more impact and push the model into a zone where outbreaks are unlikely. The final epidemic size is more sensitive to the mosquito lifespan while the epidemic peak is more sensitive to the human infectious period.

Based on our model and its assumptions, regions of the southern United States, including Houston and Los Angeles, could be at increased risk of dengue as temperature rises. However, our models also show that some regions, such as Phoenix, may have reduced risk if temperatures become too hot to sustain an outbreak. Of the cities explored, Houston has the largest risk, and generally temperatures between 27–31˚C see the largest outbreaks in our analysis. There has already been limited dengue transmission in Houston and Florida [38, 52, 53]. As

temperatures increase we can expect most cities in the southern United States to have a higher risk for dengue. However, this is not limitless, and as temperatures increase above 31˚C, outbreaks get smaller and at 35˚C there are no outbreaks. A caveat to our results is that mosquito population dynamics also depend on water availability for their life cycle, and adult lifespans also depend on humidity. So, for example, desert regions such as Phoenix may have less potential due to low humidity. Additionally, human infrastructure and behavior impacts the size and duration of dengue outbreaks. In regions with screens, air conditioning, good sanitation and water infrastructure, and access to mosquito repellent, the potential for outbreaks is decreased.

There are several limitations to this work. First, we only consider temperature dependence and not other environmental characteristics including humidity, precipitation, and vegetation. We also only consider the impacts of temperature on the extrinsic incubation period and mosquito lifespan, but other parameters have been shown to be temperature dependent, including the mosquito to human ratio, biting rate, fecundity, egg viability, larval density, development rate, and survival [54–56]. The relationships among these biological parameters, as well as their dependencies on temperature and impacts on disease transmission, are understood to be nonlinear, and in some cases, contradictory. For example, warmer temperatures (within limits) tend to increase fecundity and decrease development times, while decreasing EIP, which tends to increase mosquito abundance and therefore disease transmission. However, warmer temperatures (within limits) can decrease adult mosquito lifespans, which can reduce or even close transmission windows [10, 21, 23]. The temperature dependence in our model and simulations is based on mean temperatures, and does not take into account diurnal fluctuations, which have been shown to impact dengue transmission [10, 57]. Additional modeling studies are needed to incorporate these complexities, and to increase the accuracy of scenario-based projections.

Our sensitivity analysis is dependent on the parameter ranges we select which, while based on values from the literature, could be inaccurate. Similarly, we choose from a uniform range across the parameters, while some parameter combinations may be more or less likely than others. In the future, we plan to incorporate humidity and/or precipitation into the models and expand temperature dependence to other parameters. It may also be important in future iterations of this work to incorporate environmental dependent parameters as distributional forms within the model, and to validate against human case counts and mosquito data across a range of temperature and humidity profiles. Our contribution provides a starting place for better capturing the impacts of temperature on multiple parameters and disease dynamics, in addition to static quantities such as the basic reproduction number.

## Supporting information

**S1 Appendix. Mathematical analysis of the stability of the model system.**
(PDF)

**S1 Fig. Four model fits to mosquito lifespan data.** Data (points) from [38–40]. All models used a cubic polynomial of temperature as the explanatory variables.
(PDF)

**S1 Table. Model equations for mosquito lifespan over time.** Data (points) from [38–40]. Models are of the form $\text{Link}(y) = \alpha_0 + \beta_1 \text{temperature} + \beta_2 \text{temperature}^2 + \beta_3 \text{temperature}^3$.
(PDF)

## Author Contributions

**Conceptualization:** Imelda Trejo, Martha Barnard, Julie A. Spencer, Kaitlyn M. Martinez.

**Data curation:** Martha Barnard.

**Formal analysis:** Imelda Trejo.

**Investigation:** Imelda Trejo, Martha Barnard, Julie A. Spencer, Jeffrey Keithley, Kaitlyn M. Martinez, Isabel Crooker, Ethan O. Romero-Severson, Carrie Manore.

**Methodology:** Imelda Trejo, Martha Barnard, Julie A. Spencer, Kaitlyn M. Martinez.

**Software:** Martha Barnard, Jeffrey Keithley.

**Supervision:** Imelda Trejo, Nicolas Hengartner, Ethan O. Romero-Severson, Carrie Manore.

**Visualization:** Martha Barnard, Julie A. Spencer.

**Writing – original draft:** Imelda Trejo, Martha Barnard, Julie A. Spencer, Ethan O. Romero-Severson, Carrie Manore.

**Writing – review & editing:** Imelda Trejo, Martha Barnard, Julie A. Spencer, Kaitlyn M. Martinez, Ethan O. Romero-Severson, Carrie Manore.

## References

1. Jain R, Sontisirikit S, Iamsirithaworn S, Prendinger H. Prediction of dengue outbreaks based on disease surveillance, meteorological and socio-economic data. BMC infectious diseases. 2019; 19(1):1–16. https://doi.org/10.1186/s12879-019-3874-x PMID: 30898092
2. WHO. Dengue and severe dengue. 2021 [cited 15 October 2021]. Available from: https://www.who.int/en/news-room/fact-sheets/detail/dengue-and-severe-dengue.
3. Bhatt S, Gething PW, Brady OJ, Messina JP, Farlow AW, Moyes CL, et al. The global distribution and burden of dengue. Nature. 2013; 496(7446):504–507. https://doi.org/10.1038/nature12060 PMID: 23563266
4. Halstead SB. Which dengue vaccine approach is the most promising, and should we be concerned about enhanced disease after vaccination? There is only one true winner. Cold Spring Harbor perspectives in biology. 2018; 10(6):a030700. https://doi.org/10.1101/cshperspect.a030700 PMID: 28716893
5. Colón-González FJ, Fezzi C, Lake IR, Hunter PR. The effects of weather and climate change on dengue. PLoS Negl Trop Dis. 2013; 7(11):e2503. https://doi.org/10.1371/journal.pntd.0002503 PMID: 24244765
6. Takahashi LT, Maidana NA, Ferreira WC, Pulino P, Yang HM. Mathematical models for the Aedes aegypti dispersal dynamics: travelling waves by wing and wind. Bulletin of mathematical Biology. 2005; 67(3):509–528. https://doi.org/10.1016/j.bulm.2004.08.005 PMID: 15820740
7. Manore CA, Hickmann KS, Xu S, Wearing HJ, Hyman JM. Comparing dengue and chikungunya emergence and endemic transmission in A. aegypti and A. albopictus. Journal of theoretical biology. 2014; 356:174–191. https://doi.org/10.1016/j.jtbi.2014.04.033 PMID: 24801860
8. Mordecai EA, Caldwell JM, Grossman MK, Lippi CA, Johnson LR, Neira M, et al. Thermal biology of mosquito-borne disease. Ecology letters. 2019; 22(10):1690–1708. https://doi.org/10.1111/ele.13335 PMID: 31286630
9. Butterworth MK, Morin CW, Comrie AC. An analysis of the potential impact of climate change on dengue transmission in the southeastern United States. Environmental health perspectives. 2017; 125 (4):579–585. https://doi.org/10.1289/EHP218 PMID: 27713106
10. Robert MA, Christofferson RC, Weber PD, Wearing HJ. Temperature impacts on dengue emergence in the United States: Investigating the role of seasonality and climate change. Epidemics. 2019; 28:100344. https://doi.org/10.1016/j.epidem.2019.05.003 PMID: 31175008
11. Tun-Lin W, Burkot T, Kay B. Effects of temperature and larval diet on development rates and survival of the dengue vector Aedes aegypti in north Queensland, Australia. Medical and veterinary entomology. 2000; 14(1):31–37. https://doi.org/10.1046/j.1365-2915.2000.00207.x PMID: 10759309
12. Christofferson RC, Mores CN. Potential for extrinsic incubation temperature to alter interplay between transmission potential and mortality of dengue-infected Aedes aegypti. Environmental health insights. 2016; 10:EHI–S38345. https://doi.org/10.4137/EHI.S38345 PMID: 27478382

13. Esteva L, Yang HM. Assessing the effects of temperature and dengue virus load on dengue transmission. Journal of Biological Systems. 2015; 23(04):1550027. https://doi.org/10.1142/S0218339015500278

14. Chan M, Johansson MA. The incubation periods of dengue viruses. PloS one. 2012; 7(11):e50972. https://doi.org/10.1371/journal.pone.0050972 PMID: 23226436

15. Xiao FZ, Zhang Y, Deng YQ, He S, Xie HG, Zhou XN, et al. The effect of temperature on the extrinsic incubation period and infection rate of dengue virus serotype 2 infection in Aedes albopictus. Archives of virology. 2014; 159(11):3053–3057. https://doi.org/10.1007/s00705-014-2051-1 PMID: 24990415

16. Watts DM, Burke DS, Harrison BA, Whitmire RE, Nisalak A. Effect of temperature on the vector efficiency of Aedes aegypti for dengue 2 virus. Army Medical Research Inst of Infectious Diseases Fort Detrick MD; 1986.

17. Patz JA, Martens W, Focks DA, Jetten TH. Dengue fever epidemic potential as projected by general circulation models of global climate change. Environmental health perspectives. 1998; 106(3):147–153. https://doi.org/10.1289/ehp.98106147 PMID: 9452414

18. Kamiya T, Greischar MA, Wadhawan K, Gilbert B, Paaijmans K, Mideo N. Temperature-dependent variation in the extrinsic incubation period elevates the risk of vector-borne disease emergence. Epidemics. 2020; 30:100382. https://doi.org/10.1016/j.epidem.2019.100382

19. Tjaden NB, Thomas SM, Fischer D, Beierkuhnlein C. Extrinsic incubation period of dengue: knowledge, backlog, and applications of temperature dependence. PLoS neglected tropical diseases. 2013; 7(6): e2207. https://doi.org/10.1371/journal.pntd.0002207 PMID: 23826399

20. Rohani A, Wong Y, Zamre I, Lee H, Zurainee M, et al. The effect of extrinsic incubation temperature on development of dengue serotype 2 and 4 viruses in Aedes aegypti (L.). Southeast Asian Journal of Tropical Medicine and Public Health. 2009; 40(5):942. PMID: 19842378

21. Mordecai EA, Cohen JM, Evans MV, Gudapati P, Johnson LR, Lippi CA, et al. Detecting the impact of temperature on transmission of Zika, dengue, and chikungunya using mechanistic models. PLoS neglected tropical diseases. 2017; 11(4):e0005568. https://doi.org/10.1371/journal.pntd.0005568 PMID: 28448507

22. Mordecai EA, Paaijmans KP, Johnason LR, Balzer C, Ben-Horin T, de Moor E, et al. Optimal temperature for malaria transmission is dramatically lower than previously predicted. Ecology letters. 2013; 16 (1):22–30. https://doi.org/10.1111/ele.12015 PMID: 23050931

23. Shocket MS, Verwillow AB, Numazu MG, Slamani H, Cohen JM, El Moustaid F, et al. Transmission of West Nile and five other temperature mosquito-borne viruses peaks at temperatures between 23 C and 26 C. eLife. 2020; 9:e58511. https://doi.org/10.7554/eLife.58511 PMID: 32930091

24. Johnson LR, Ben-Horin T, Lafferty KD and McNally A, Mordecai E and Paaijmans Krijn P, et al. Understanding uncertainty in temperature effects on vector-borne disease: a Bayesian approach Ecology. 2015; 96(1):203–213. https://doi.org/10.1890/13-1964.1 PMID: 26236905

25. Paull SH, Horton DE, Ashfaq M, Rastogi D, Kramer LD, Diffenbaugh NS, et al. Drought and immunity determine the intensity of west nile virus epidemics and climate change impacts Proceedings of the Royal Society B: Biological Sciences. 2017; 284(1848):20162078. https://doi.org/10.1098/rspb.2016.2078 PMID: 28179512

26. Mayton EH, Ryan TA, Wearing JG, Christofferson RC Age-structured vectorial capacity reveals timing, not magnitute of within-mosquito dynamics is critical for arbovirus fitness assessment BioMed Central. 2020: 13(1):1–13. https://doi.org/10.1186/s13071-020-04181-4 PMID: 32539759

27. Hahn MB, Eisen L, McAllister J, Savage HM, Mutebi JP, Eisen RJ. Updated reported distribution of Aedes (stegomyia) aegypti and Aedes (stegomyia) albopictus (diptera: Culicidae) in the United States, 1995–2016. Journal of medical entomology. 2017; 54(5):1420–1424. https://doi.org/10.1093/jme/tjx088 PMID: 28874014

28. Reinhold JM, Lazzari CR, Lahondère C. Effects of the environmental temperature on Aedes aegypti and Aedes albopictus mosquitoes: a review. Insects. 2018; 9(4):158. https://doi.org/10.3390/insects9040158 PMID: 30404142

29. Morin CW, Monaghan AJ, Hayden MH, Barrera R, Ernst K. Meteorologically driven simulations of dengue epidemics in San Juan, PR. PLoS neglected tropical diseases. 2015; 9(8):e0004002. https://doi.org/10.1371/journal.pntd.0004002 PMID: 26275146

30. Andraud M, Hens N, Marais C, Beutels P. Dynamic epidemiological models for dengue transmission: a systematic review of structural approaches. PloS one. 2012; 7(11):e49085. https://doi.org/10.1371/journal.pone.0049085 PMID: 23139836

31. CDC. Human disease cases. Reported to CDC ArboNET by county of residence. Dengue Virus (Locally Acquired). 2021 [cited 23 July 2022]. Available from: https://wwwn.cdc.gov/arbonet/Maps/ADB_Diseases_Map/index.html.

32. Manzin A, Martina BE, Gould EA, Bagnarelli P, Sambri V. Human arthropod-borne viral infections. BioMed Research International. 2013 ( 2013). https://doi.org/10.1155/2013/608510 PMID: 24455709

33. Chitnis N, Cushing JM, Hyman J. Bifurcation analysis of a mathematical model for malaria transmission. SIAM Journal on Applied Mathematics. 2006; 67(1):24–45. https://doi.org/10.1137/050638941

34. Morita Y, Kogure H, Sandoh M, Kawashima G, Sato Y, Nanba S, et al. An imported dengue fever case by dengue virus 3 (DENV-3) infection in Gunma, Japan Japanese journal of infectious diseases. 2008; 61(1):90. PMID: 18219146

35. Gubler DJ. Dengue and dengue hemorrhagic fever. Clinical microbiology reviews. 1998; 11(3):480–496. https://doi.org/10.1128/cmr.11.3.480 PMID: 9665979

36. Reich NG, Shrestha S, King AA, Rohani P, Lessler J, Kalayanarooj S, et al. Interactions between serotypes of dengue highlight epidemiological impact of cross-immunity. Journal of The Royal Society Interface. 2013; 10(86):20130414. https://doi.org/10.1098/rsif.2013.0414 PMID: 23825116

37. Ngwa GA, Shu WS. A mathematical model for endemic malaria with variable human and mosquito populations. Mathematical and computer modelling. 2000; 32(7-8):747–763. https://doi.org/10.1016/S0895-7177(00)00169-2

38. Yang HM, Macoris MD, Galvani KC, Andrighetti MT, Wanderley DM. Assessing the effects of temperature on the population of Aedes aegypti, the vector of dengue. Epidemiology and Infection. 2009; 137 (8):1188–1202. https://doi.org/10.1017/S0950268809002052 PMID: 19192322

39. Beserra E, Fernandes C, Silva S, Silva L, Santos J. Effects of temperature on life cicle, thermal exigency and number of generations per year estimation of Aedes aegypti (Diptera, Culicidae). Iheringia Série Zoologia. 2009; 99:142–148. https://doi.org/10.1590/S0073-47212009000200004

40. Hamdan N, Kilicman A. The effect of temperature on mosquito population dynamics of Aedes aegypti: The primary vector of dengue. In: AIP Conference Proceedings. vol. 2266. AIP Publishing LLC; 2020. p. 050002.

41. Hattab MW. A derivation of prediction intervals for gamma regression. Journal of Statistical Computation and Simulation. 2016; 86(17):3512–3526. https://doi.org/10.1080/00949655.2016.1169421

42. National Centers for Environmental Information. Climate at a Glance: City Time Series. 2021 [cited 6 January 2021]. Available from: https://www.ncdc.noaa.gov/cag/.

43. Van den Driessche P, Watmough J. Reproduction numbers and sub-threshold endemic equilibria for compartmental models of disease transmission. Mathematical biosciences. 2002; 180(1-2):29–48. https://doi.org/10.1016/S0025-5564(02)00108-6 PMID: 12387915

44. Hethcote HW. The mathematics of infectious diseases. SIAM review. 2000; 42(4):599–653. https://doi.org/10.1137/S0036144500371907

45. McKay M, Beckman R, Conover W. Comparison the three methods for selecting values of input variable in the analysis of output from a computer code. Technometrics;(United States). 1979; 21(2).

46. Marino S, Hogue IB, Ray CJ, Kirschner DE. A methodology for performing global uncertainty and sensitivity analysis in systems biology. Journal of theoretical biology. 2008; 254(1):178–196. https://doi.org/10.1016/j.jtbi.2008.04.011 PMID: 18572196

47. Saltelli A, Tarantola S, Chan KPS. A quantitative model-independent method for global sensitivity analysis of model output. Technometrics. 1999; 41(1):39–56. https://doi.org/10.1080/00401706.1999.10485594

48. Thavara U, Tawatsin A, Chansang C, Kong-ngamsuk W, Paosriwong S, Boon-Long J, et al. Larval occurrence, oviposition behavior and biting activity of potential mosquito vectors of dengue on Samui Island, Thailand. Journal of Vector Ecology. 2001; 26:172–180. PMID: 11813654

49. Massad E, Amaku M, Coutinho FAB, Struchiner CJ, Lopez LF, Wilder-Smith A, et al. Estimating the size of Aedes aegypti populations from dengue incidence data: implications for the risk of yellow fever outbreaks. Infectious Disease Modelling. 2017; 2(4):441–454. https://doi.org/10.1016/j.idm.2017.12.001 PMID: 30137722

50. Coutinhoa F, Burattinia M, Lopeza L, Massada E. Threshold conditions for a non-autonomous epidemic system describing the population dynamics of dengue. Bulletin of mathematical biology. 2006; 68 (8):2263–2282. https://doi.org/10.1007/s11538-006-9108-6

51. Wikipedia. Metropolitan statistical area 2022 [cited 20 December 2022]. Available from: https://en.wikipedia.org/wiki/Metropolitan_statistical_area.

52. Radke EG, Gregory CJ, Kintziger KW, Sauber-Schatz EK, Hunsperger EA, Gallagher GR, et al. Dengue outbreak in key west, Florida, USA, 2009. Emerging infectious diseases. 2012; 18(1):135. https://doi.org/10.3201/eid1801.110130 PMID: 22257471

53. Murray KO, Rodriguez LF, Herrington E, Kharat V, Vasilakis N, Walker C, et al. Identification of dengue fever cases in Houston, Texas, with evidence of autochthonous transmission between 2003 and 2005.

Vector-Borne and Zoonotic Diseases. 2013; 13(12):835–845. https://doi.org/10.1089/vbz.2013.1413 PMID: 24107180

54. Christofferson RC, Wearing HJ, Walsh CD, Salje H, Kiem CT, Cauchemez S. How do I bite thee? Let me count the ways: Heterogeneity and temperature dependence in Ae. aegypti biting habits drive individual mosquito arbovirus transmission potential. bioRxiv. 2021.

55. Zapletal J, Erraguntla M, Adelman ZN, Myles KM, Lawley MA Impacts of diurnal temperature and larval density on aquatic develompent of Aedes aegypti. PLoS One 2018; 13(3):e0194025 https://doi.org/10.1371/journal.pone.0194025 PMID: 29513751

56. Costa EAPDA, Santos EMDM, Correia JC, Albuquerque CMRD Impact of small variations in temperature and humidity on the reproductive activity and survival of Aedes aegypti (Diptera, Culicidae). Revista Brasileira de Entomologia 2018; 54:488–493. https://doi.org/10.1590/S0085-56262010000300021

57. Carrington LB, Armijos MV, Lambrechts L, Scott TW. Fluctuations at a low mean temperature accelerate dengue virus transmission by Aedes aegypti. PLoS neglected tropical diseases. 2013; 7(4):e2190. https://doi.org/10.1371/journal.pntd.0002190 PMID: 23638208